THE AMERICAN MINERALOGIST, VOL. 47, JULY–AUGUST, 1962

PETROGRAPHIC CHARACTERISTICS OF YOUNG SEA ICE, POINT BARROW, ALASKA

W. F. WEEKS[1] AND W. L. HAMILTON, *Materials Research Branch, Cold Regions Research and Engineering Laboratory, Hanover, New Hampshire.*

ABSTRACT

A pilot study is made of interrelations between structural features readily observed in horizontal thin sections of sea ice under low magnification. The core used was 31.4 cm in length and was collected from Elson Lagoon, Point Barrow, Alaska on 26 October, 1960. The growth of the ice sheet from its formation on 1 October to the time of sampling can be described by $Z=1.20\ (S+\Sigma\theta)^{0.60}$ where Z is the thickness of the ice sheet in cm, $\Sigma\theta$ is the accumulated degree days, and S is a fictitious number of degree days, in this case, 38, assigned to the initial conglomeration of slush ice. Important intercrystalline structural features are a systematic increase in crystal size with depth and a fairly constant 2:1 ratio between the length and width of the ice crystals. Comparisons are made with recent observations on crystal growth in metals. The frequency distributions of plate widths, a, the distance between the centers of adjacent subgrains measured parallel to the c-axes of the ice crystals, commonly show significant positive skews. The average value of a shows a slight but significant increase with increasing depth in the ice sheet. Within the limited range of observations a strong linear correlation ($r=-0.95$) exists between $\bar{a}$ and v, the growth velocity in mm/hr: $\bar{a}=0.70-0.10\ v$. This relation however will not explain observations at either low or high growth rates. Plots of sub-plate widths vs subplate lengths show an extreme scatter and a slight increase in the modal value of the plate length with increasing plate width. The packings of the sub-plates in sea ice are compared with packings observed in zinc and are found to be similar.

INTRODUCTION

That the inter- and intracrystalline structure of sea ice is important in controlling the large variation in the physical properties of sea ice is well known (Anderson and Weeks, 1958; Assur, 1958; Anderson, 1960). However, detailed measurements of structural parameters are almost completely lacking; it is usually assumed that they are constant throughout a given sheet of sea ice. The following paper is a pilot study of those structural features observed readily with low magnification in thin sections of natural sea ice. No attempt has been made to study the shapes and distributions of brine pockets.

The sea ice sheet described here formed on Elson Lagoon at Point Barrow, Alaska, in the period between 30 September and 26 October 1960. The initial ice development consisted of the formation of a layer of loose frazil crystals and slush pancakes. On 1 October the ice sheet had stabilized forming a pan agglomerate, and the slush layer was approxi-

[1] Academic Address: Department of Geology, Dartmouth College, Hanover, New Hampshire.

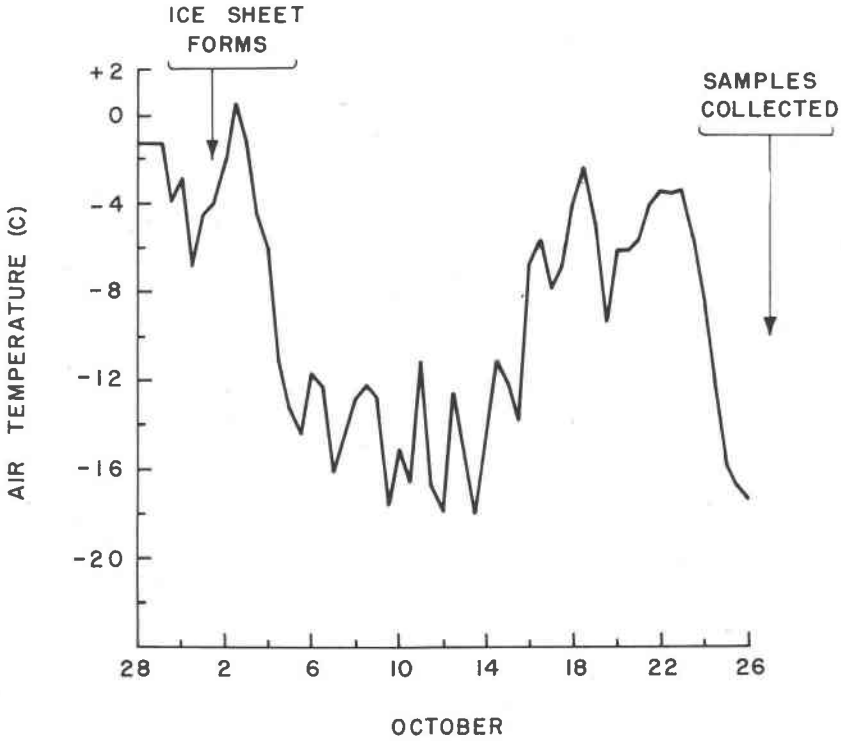

FIG. 1. Air temperatures (noon and midnight) Point Barrow, Alaska, from 28 Sept. to 26 Oct. 1960.

mately 7.6 cm thick. After this initial sheet formed, an orderly sea ice growth pattern developed.

A temperature record for this period is presented in Figure 1. Noon and midnight temperature measurements were taken from the records of the U. S. Weather Bureau station at Barrow Village. Although Barrow Village is approximately 9 miles southwest of the sea ice test site, comparison of this data with spot temperature measurements taken at the test site is good.

Average ice thicknesses in the near vicinity of the test site are shown in Fig. 2. The large scatter in the data reflects local insulating effects of snow drifts formed near foreign objects lying on the ice surface and the areal disperion of measurements over the test site. Because of the initial period of slush formation before the ice sheet solidified, the ice thickness at time zero (1 October) was approximately 7.6 cm.

If the slush ice is considered as being present when the ice growth

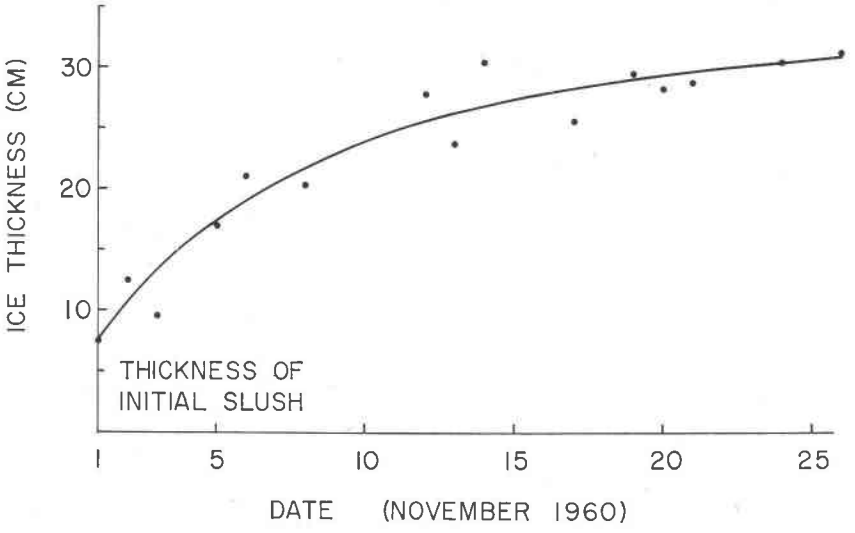

FIG. 2. Sea ice thickness vs date of measurement.

started and 1 accumulated degree day is set equal to 7.6 cm of sluch ice, the field data are well fitted by the relation $Z=7.60\ (\Sigma\theta)^{0.26}$ where Z is the thickness of the ice in the vicinity of the test area and $\Sigma\theta$ the number of accumulated degree days measured after time zero (Fig. 3). This relation is, however, not comparable with other empirical ice growth equations since the initial slush ice is not the result of growth but of conglomeration over a period of several days. This may be corrected by arbitrarily assigning a fictitious number of degree days, S, to the initial slush thickness using the relation $Z=a(S+\Sigma\theta)^k$ where a and k are empirical constants. If these values are assumed to be 1.33 and 0.58 respectively based on the measurements of Lebedev (1938) in the Russian Arctic, S can be estimated as approximately 38 degree days. Now setting $\Sigma\tilde{\theta}=S+\Sigma\theta$ the relation $Z=1.20\ (\Sigma\tilde{\theta})^{0.60}$ can be obtained by least squares from the Point Barrow data. It is interesting to note that the power 0.60 although slightly lower is in the same range, 0.70, as observed for 10 to 30 cm thick sea ice at Thule, Greenland (Anderson, 1961). Since density measurements taken with a bulb hydrometer showed a salinity of 31°/₀₀ for Elson Lagoon water before the ice sheet formed, accumulated degree days were calculated relative to -1.7 C.

On 26 October, a 3 in vertical ice core was cut with a CRREL ice auger at a point approximately 100 m from the shore. Snow accumulation at the immediate site of the sample was 5 cm. The salinity profile

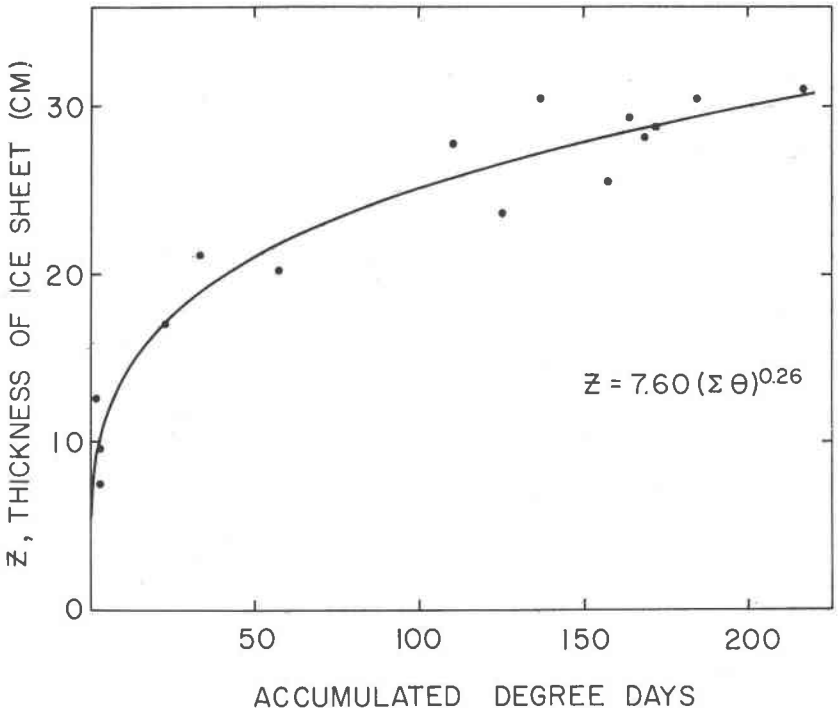

FIG. 3. Sea ice thickness vs accumulated degree days referenced to −1.7 C.

of this core can be estimated from salinity measurements on cores taken from the vicinity of the test sample on 25, 26, and 29 October (Fig. 4). With the exception of high salinity values from the slush ice, the salinity is essentially constant with depth. There is no systematic change in the salinity profiles taken on different dates.

The core, which measured 31.4 cm, was immediately removed from the auger, freed of loose slush, and stored upright in an outdoor laboratory away from direct sunlight. On 28 October, with air temperature at −12.9 C., the core was cut into a series of thin sections with an electric band saw. In assigning the thin sections to their proper sequence in the ice sheet, a total error of only 0.35 cm was accumulated. Thin sections varied from 0.25 to 0.75 cm in thickness. The thin sections were then transferred to a floor freezer with an ambient temperature of -17.5 ± 0.5 C. Photographs were made in a walk-in freezer at −11 to −12 C. Final photographs were taken on 1 December. Two photographs were made of each thin section, one with transmitted light and the other using crossed polaroids. In general, the photographs using crossed polaroids delineated

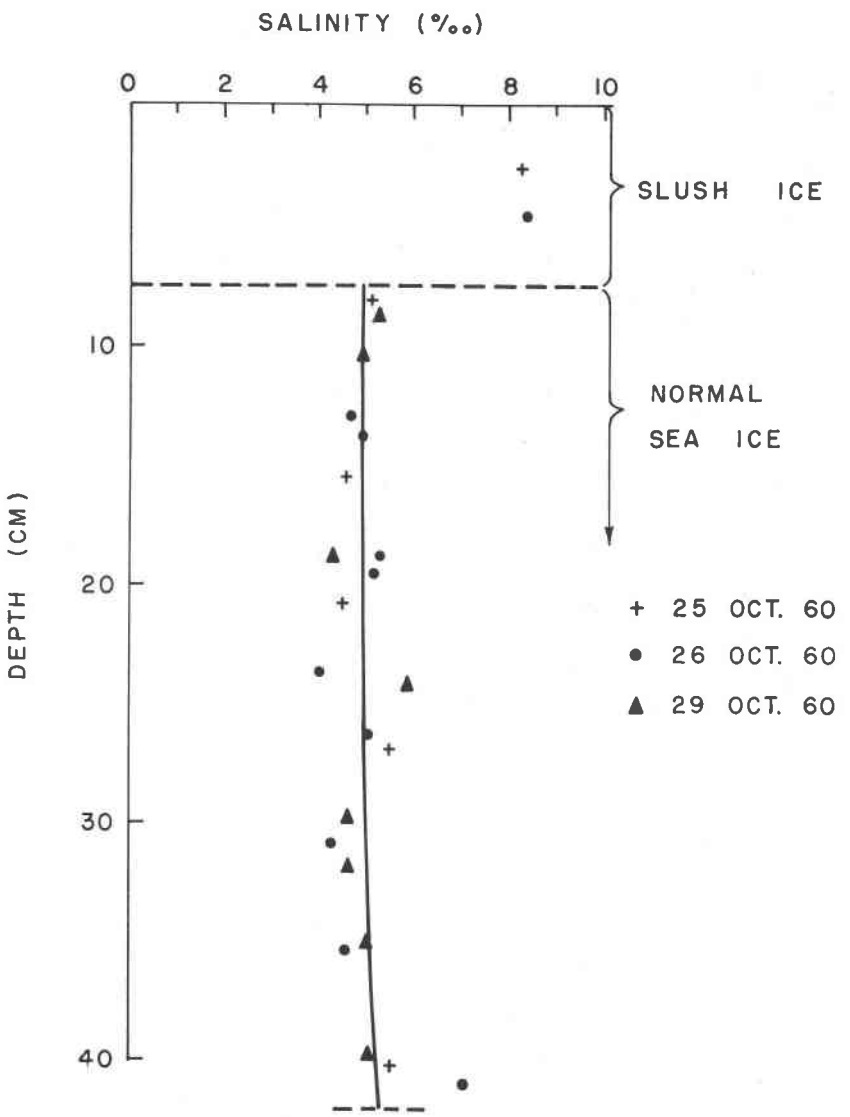

FIG. 4. Ice salinity profiles taken in the test area between 25 and 29 October, 1960.

the crystal and subgrain structures much more clearly. Enlargements ranging from 33 to 57 were made from the negatives. The data presented in this paper were obtained by direct measurements on these photo enlargements.

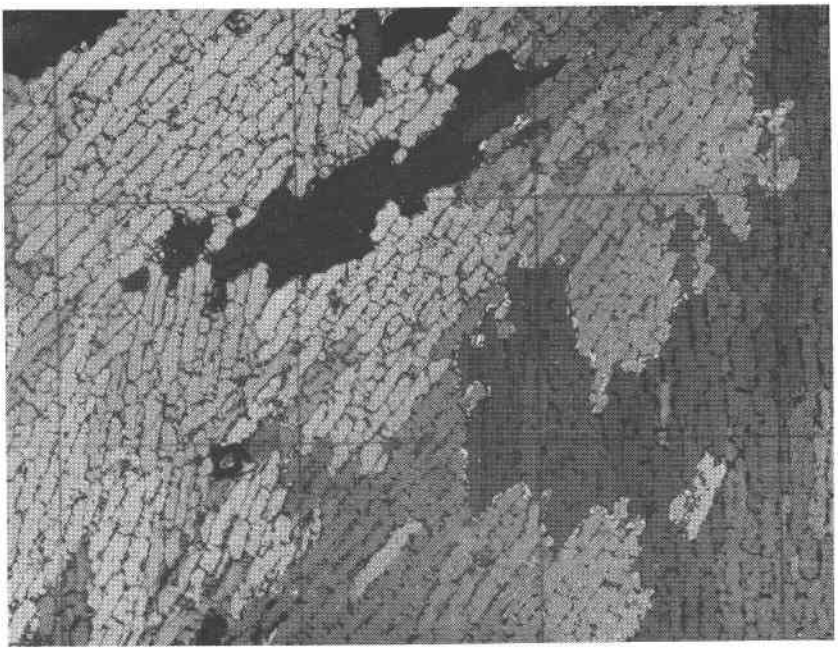

FIG. 5. Photomicrograph of horizontal thin section of sea ice from 27.9 cm below the upper surface of the ice sheet. The grid is 1 cm on a side.

PETROGRAPHIC CHARACTERISTICS

Intercrystalline features

Figure 5 is a photomicrograph from the 27.9 cm level of the ice core showing the well developed macro-mosaic structure so characteristic of natural sea ice. Each sea ice crystal is composed of a number of sub-grains of pure ice that are separated by small-angle grain boundaries along which films and pockets of brine are localized. The sub-grains are usually elongated in a direction parallel to the (0001) plane. Since each sub-grain represents an ice platelet that grew into the underlying sea water, the (0001) elongation is produced by a slower crystal growth perpendicular to the basal plane than parallel to it. As shown in Fig. 5, single crystals of sea ice are easily delineated under crossed polaroids because they behave as extinction units. Although no universal stage measurements were made on this ice, it is evident that, since the planes of brine inclusions show an essentially vertical pattern in horizontal thin sections, the *c*-axes will lie in the horizontal plane. If there is no preferred pattern to the distribution of *c*-axes in this plane, the ice under study will show a horizontal girdle on an equal area projection similar to the girdle ob-

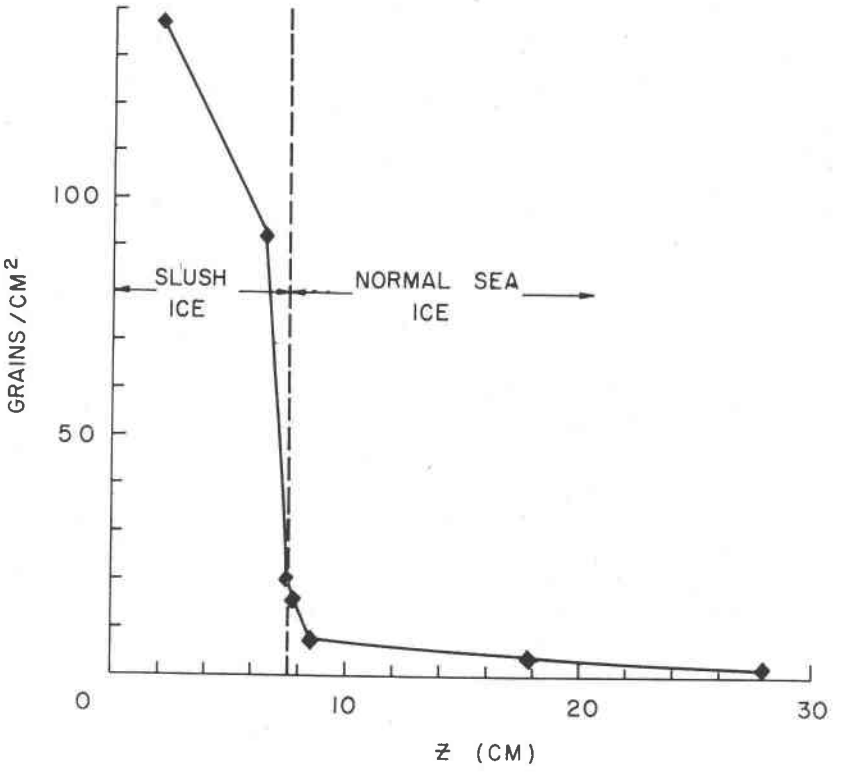

FIG. 6. Increase in crystal size with Z, distance below ice sheet surface.

served in sea ice at Hopedale, Laborador, by Weeks and Lee (1958, Fig. 7, p. 141).

The most pronounced effect observed in the study of the photomicrographs is the increase in crystal size as a function of depth below the surface of the ice sheet. The number of crystals per square centimeter at several different levels in the ice sheet was determined by counting the crystals in a planimetered area. Results are shown in Fig. 6. Similar grain coarsening effects are well known in metals, and the fine-grained slush ice and normal sea ice observed at Point Barrow can be compared directly to the chill and columnar zones of metal castings described by Walton and Chalmers (1959). The chill zone consists of small crystals that are relatively equidimensional and apparently random in orientation while the columnar zone consists of much larger crystals that are elongated parallel to the direction of heat flow and show a strong preferred orientation. Examination of vertical thin sections shows that there

is a sharp change in the number of grains/cm^2 at the slush-normal sea ice boundary and a gradual increase in the average grain size with depth in both slush and normal sea ice.

Figure 7 shows the maximum width, W, of a number of crystals plotted against the maximum length, L. Length measurements were always taken parallel to the (0001) plane and width measurements normal to this direction (parallel to the c-axis). The 0.95 confidence bands for $\hat{\beta}_0$ and $\hat{\beta}_1$, the estimated intercept and slope, are ± 0.400 and ± 0.605 respectively. These limits enclose $\beta_0 = 0$ and $\beta_1 = 2$ so that these could be assumed as population parameters within the error limit. A ($\beta_0 = 0$) value is quite reasonable since it is logical that zero crystal length would be proportional to zero crystal width. The $\beta_1 = 2$ value is very interesting in view of recent work on growth anisotropy in ice by Hillig (1958) and the observation by Hallett (1960) that, in meltwater pools, ice dendrites commonly form with a [growth parallel to the (0001) plane/growth perpendicular to (0001) plane] ratio of roughly 100/1. The observed 2/1 ratio indicates that the rates of sidewise and edgewise growth of the colonies of sub-grains that combine together to make up the single crystals do not differ nearly as much as might be expected. How sea ice crystals grow sidewise at such appreciable velocities is not understood at the present, particularly since, during this growth, the crystals apparently systematically "incorporate" small-angle boundaries containing brine inclusions at regular intervals in the (0001) plane, *i.e.*, parallel to the crystal-melt interface. Similar observations of the relative magnitude of lengthwise and sidewise growth have been reported from studies of pearlitic growth phenomena in Fe-Mo-C alloys (Mehl and Hagel, 1956).

Intracrystalline features

The most obvious vertical change in the intracrystalline features of the Point Barrow sea ice is the marked decrease in definition of the small-angle sub-grain boundaries in the upper part of the normal sea ice. This results from the brine being localized into a few separated pockets. Since at low magnification the small-angle sub-boundaries are revealed only by the presence of brine pockets, the boundaries are poorly delineated, making accurate measurements difficult. In particular it is difficult to measure the lengths of the sub-plates since the plate terminations are especially poorly defined. In the lower portion of the columnar ice, below approximately 17 cm, both plate widths and lengths can readily be measured.

The distance between the centers of adjacent sub-grains, measured parallel to the c-axis, will be referred to as a, the plate or sub-grain

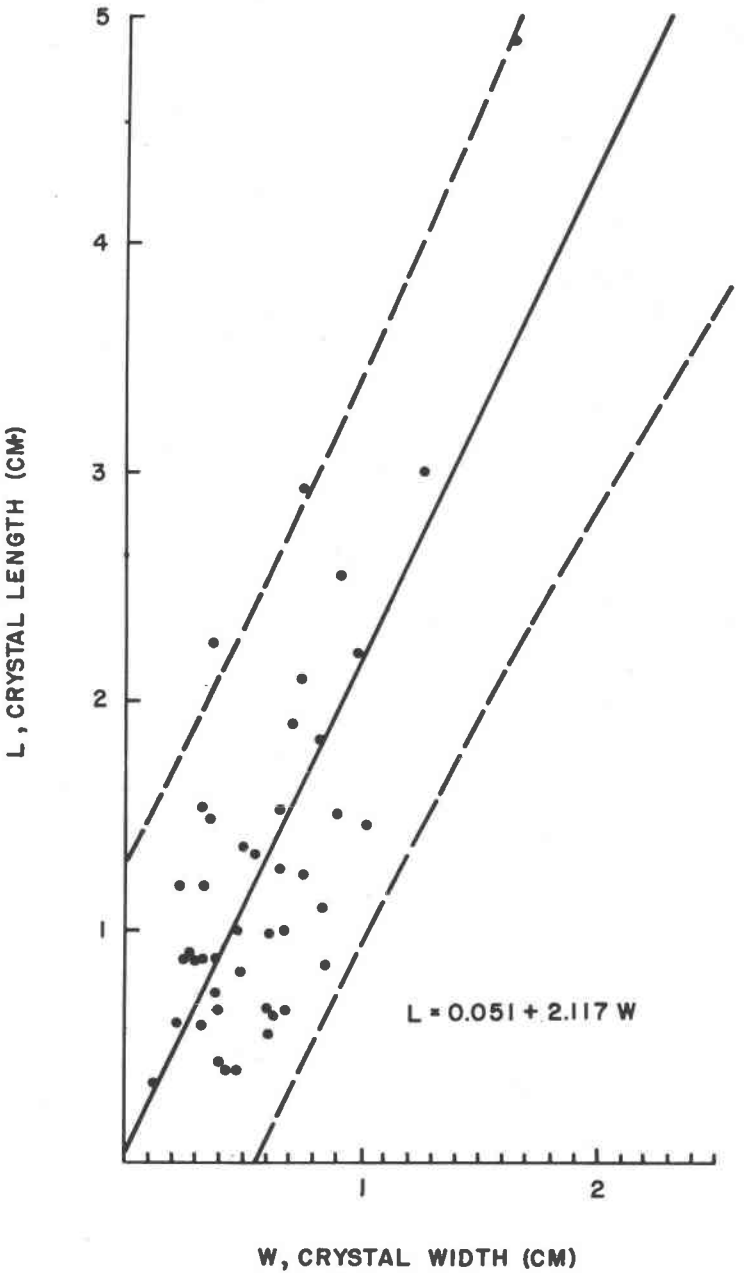

FIG. 7. Crystal width vs crystal length. All measurements from horizontal thin sections.

width. Measurement of this quantity is commonly a bit subjective. In this paper an attempt was made to measure the average width of each plate. The length of each plate, perpendicular to the c-axis, was also measured and designated as b. All resolvable plates within a given crystal were measured before moving on to the next crystal. It was thought that this would minimize the tendency to select prominent plates.

Frequency histograms of the distributions of plate widths at several different levels are presented in Fig. 8. Table 1 gives the summary statistics. Several of these distributions show a positive skewness greater than would be expected at the 0.95 level of significance from a random sample drawn from a normally distributed population. This positive skewness cannot be explained by the inclusion of crystals with significantly non-horizontal c-axes (deviations of $>25°$) in the sample since Weeks and Assur (1962) found similar plate-width distributions in NaCl ice 30 cm below the initial ice surface, where all the crystals were known to have horizontally oriented c-axes.

A less apparent variation in plate structure is the gradual net increase in the plate width a, with increasing depth in the ice sheet. That such a variation in plate width should occur in natural sea ice has been suggested by studies of substructures in NaCl ice crystals (Weeks, 1962) and metals (Elbaum, 1959). That the expected variation in plate width actually occurs, however, has not yet been demonstrated. Figure 9 presents the average plate widths measured on the Point Barrow sea ice plotted against depth in the ice sheet. A linear least-squares fit of this data is:

$$\bar{a} = 0.5136 + 0.0052\,Z$$

TABLE 1. SUMMARY STATISTICS OF PLATE-WIDTH FREQUENCY DISTRIBUTIONS

Distance below ice surface, z (cm)	Plate type	Avg. plate width $\bar{a}$ (mm)	Standard deviation s	$\sqrt{\beta_1}$	β_2	n
9.0	Secondary	0.376	0.129	+0.421[1]	3.331	100
9.5	Secondary	0.438	0.124	+0.217	3.033	70
9.5	Primary	0.584	0.166	+0.794[1]	4.734	101
12.1	Primary	0.560	0.210	+0.630[1]	3.761[1]	200
21.8	Primary	0.636	0.150	−0.063	2.915	200
28.3	Primary	0.617	0.127	+0.261	3.085	200
29.8	Primary	0.711	0.209	+0.719[1]	2.780	200

[1] Indicates significance at the 0.95 probability level.

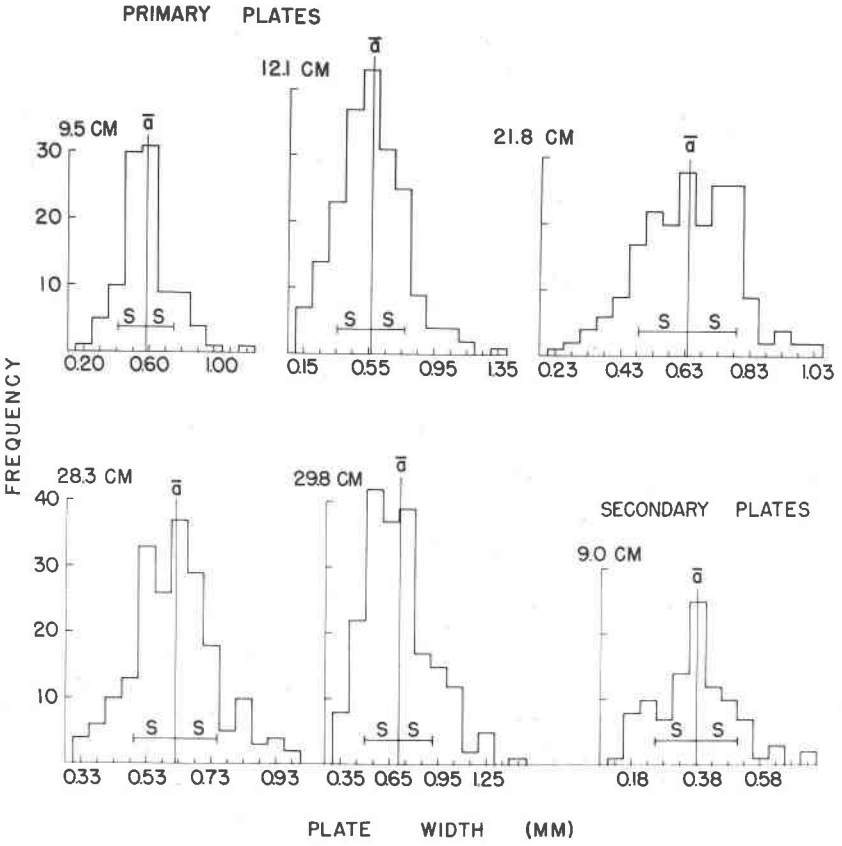

FIG. 8. Frequency histograms of a, plate or grain width in mm, at different depths below the ice sheet surface ($\bar{a}$ and s indicate sample mean and standard deviation respectively). Primary plates are from normal sea ice. Secondary plates represent a distinct type probably produced by refreezing.

where $\bar{a}$ is the average plate width (mm) and Z is the distance below the ice surface (cm). The 0.95 confidence intervals on $\hat{\beta}_1$, the slope estimator, are ± 0.0049. Zero is not contained within this interval so it can be concluded that the data indicates a small but significant increase in $\bar{a}$ with depth. Because of the limited range of the observations, nothing can be said about the form of the relation between $\bar{a}$ and Z.

In NaCl ice (Weeks, 1962) measurements of $\bar{a}$ and v, the growth velocity in mm/hr, fit the general equation suggested by Frank (1956), $\bar{a}\ v^{1/2} = \text{constant}$, slightly better than $\bar{a}\ v = \text{constant}$ as suggested by Teghtsoonian and Chalmers (1951). Figure 10 presents a plot of the $\bar{a}$

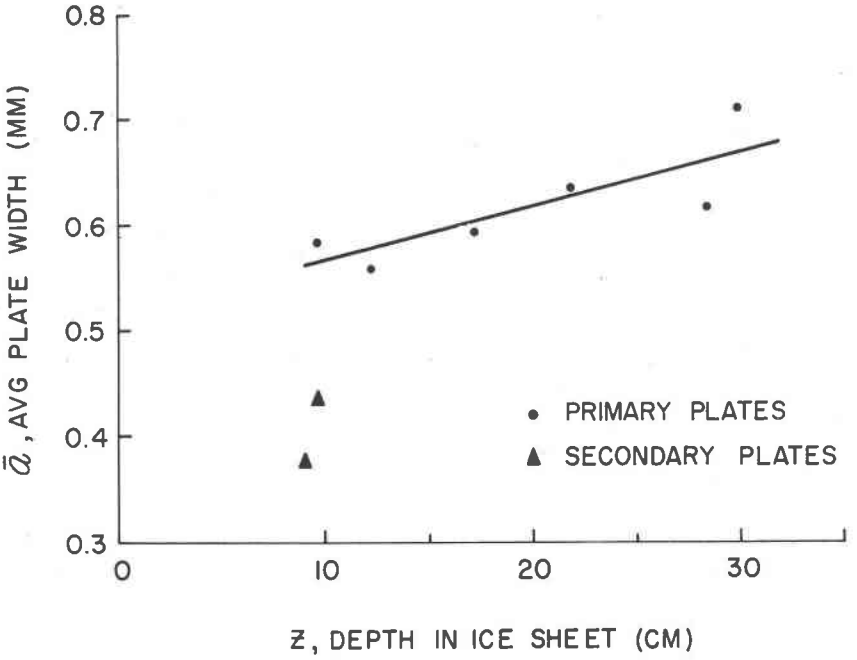

FIG. 9. Increase in $\bar{a}$, average plate width, with Z, depth below the surface of the ice sheet.

vs v data for both the NaCl ice and the Point Barrow sea ice. The best empirical fit within the range of the data appears to be linear,

$$\bar{a} = 0.70 - 0.10\,v$$

with a correlation coefficient $r = -0.95$. The sets of data appear to be continuous although the amount of actual overlap is small. It should be noted however that the accuracy in estimating v is much lower in the case of natural sea ice than for NaCl ice.

If a linear relation were to hold, this would imply that the plate width would equal zero at $v \sim 7$ mm/hr and become negative at higher growth velocities. In addition the maximum possible value of $\bar{a}$, corresponding to zero growth velocity, would be ~ 0.7 mm. There is good reason to doubt that 0.7 mm is the maximum possible value of $\bar{a}$ since values of roughly 1.0 mm are commonly observed in thick, slowly grown pack ice (Schwarzacher, 1959). Also although no information is available in the ice literature regarding plate spacings at high growth velocities, a negative plate spacing would have no physical significance. Therefore it can be concluded that, although the data presented in this paper definitely establish that $\bar{a} = f(v)$ for natural sea ice as well as NaCl ice, it is not

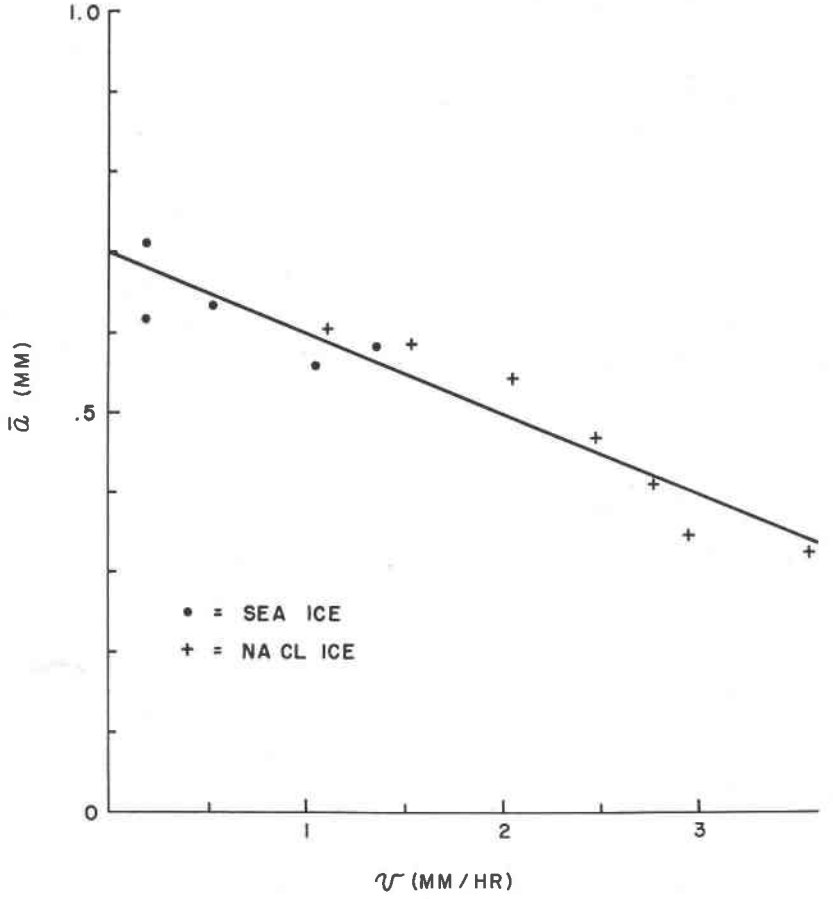

FIG. 10. Decrease in average plate width, $\bar{a}$, with increasing growth velocity, v.

possible at present to definitely establish the form of this relationship. Perhaps part of the difficulty results from assuming that sea ice and NaCl ice constitute one homogeneous set of data.

In the upper part of the core, above approximately 16.5 cm, a number of roughly circular ice areas that differed markedly from the surrounding normal sea ice were observed in horizontal thin sections. This ice forms continuous bodies that enlarge toward the top of the ice sheet and vary from 0.25 to 1.0 cm in diameter. The boundaries separating this ice from normal sea ice are quite sharp and the ice appears to have a higher salinity. The sub-platelets in this ice are very distinct and easy to measure even in thin sections from the 9.0 and 9.5 cm levels, while in the sur-

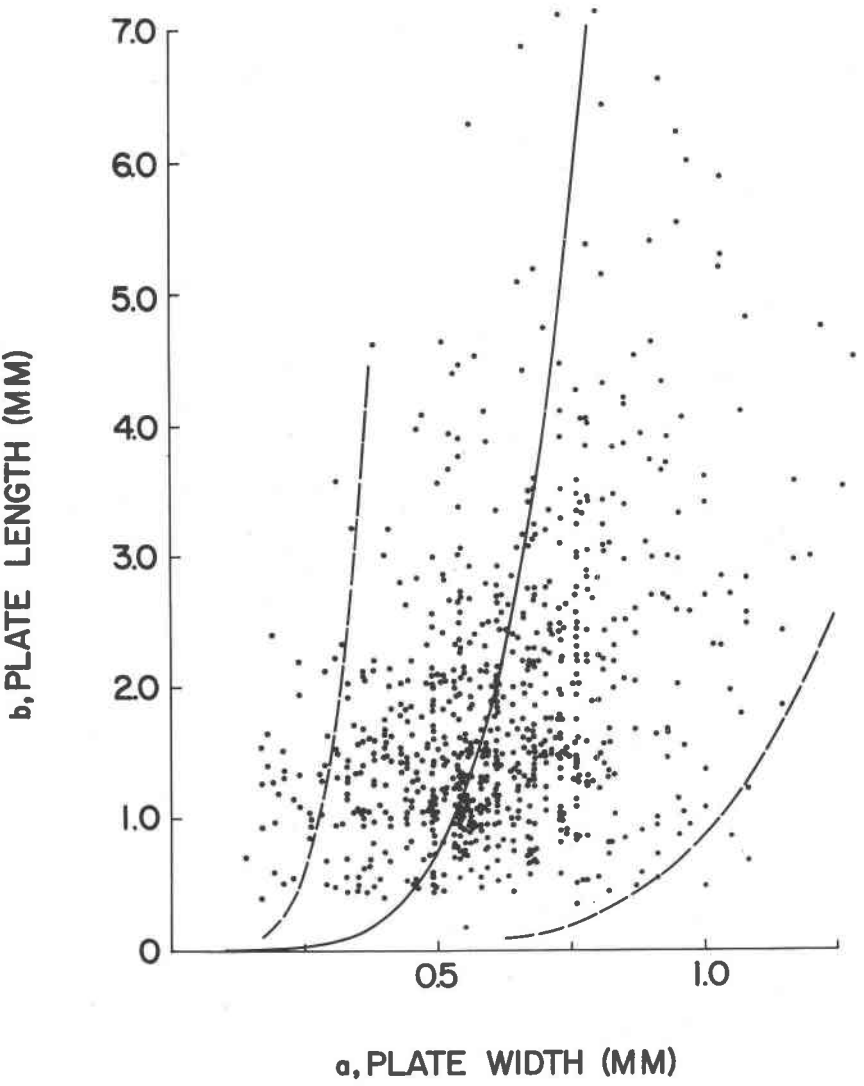

FIG. 11. Scatter diagram of sub-plate widths, a, against sub-plate lengths, b.

rounding sea ice the plates were measured with considerable difficulty. Frequency distributions of these "secondary plates" are also presented in Figure 8 and Table 1. Plate widths were found to be considerably smaller than those in the surrounding ice (Fig. 9). It is believed that this ice was produced by refreezing brine drainage channels that formed during the warm period of 18 to 23 October. When the air temperature

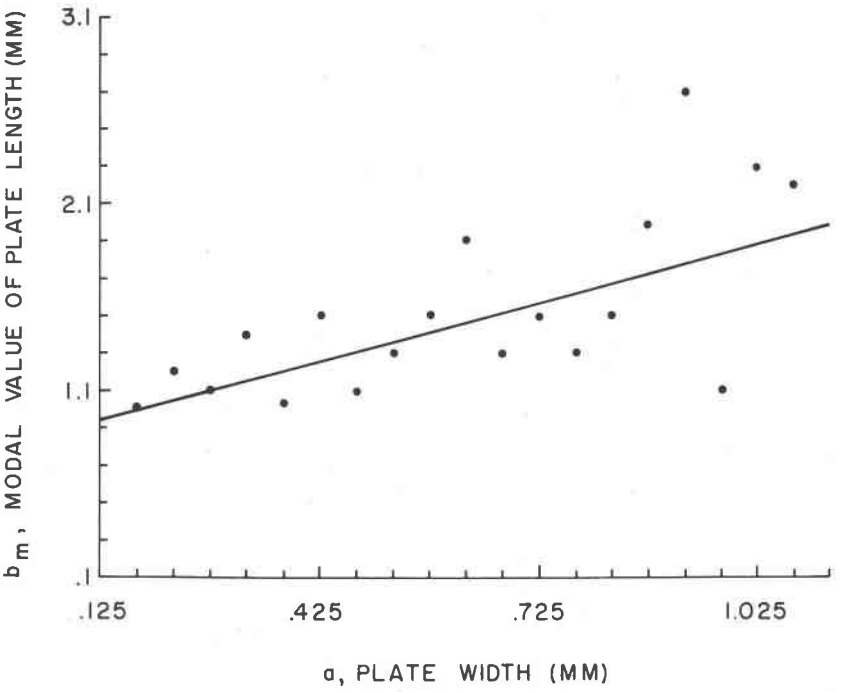

FIG. 12. Increase in modal values of plate lengths, b_m, with increasing plate width, a.

dropped suddenly on 24 October, these brine channels refroze quite rapidly producing smaller plate widths and a more saline ice. Because of their origin these plates are referred to as "secondary" in Figures 8 and 9 and Table 1.

Figure 11 presents a plot of individual plate widths a vs plate lengths b. The scatter is rather extreme and there appears to be little correlation. The fitted curve is $a=0.53b^{0.20}$. The confidence bands are at the 0.95 significance level. Visual examination of the scatter diagram shows that the b values are strongly positively skewed and that the variance of b increases with increasing a. In an attempt to avoid the influence of these factors, the data was separated into 19 class intervals of a and a modal value of b was determined from the frequency distribution in each particular class interval. In the few cases where the frequency distribution was multi-modal, the arithmetic mean of the modes was used. The data were then weighted relative to the number of measurements in each frequency distribution and a linear regression line computed. The modal values b_m and the resulting regression line $b_m=0.8105+1.0515\ a$ are presented in Figure 12. The 0.95 confidence intervals on $\hat{\beta}_1$, the slope

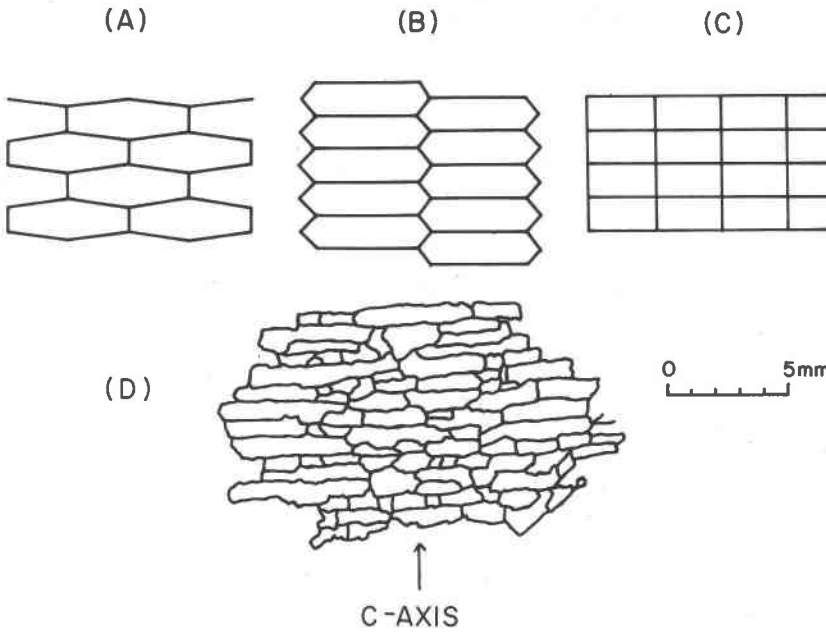

FIG. 13. Idealized sub-plate packings as observed in zinc (A, B, C) and typical sub-plate packings from Point Barrow sea ice (D).

estimator, are ± 0.3112 indicating that there is a significant increase in b_m with increasing a.

The manner in which the sub-plates are packed together is also of interest. Figure 13 shows idealized drawings of types of sub-plate packing observed in Zn, a close packed hexagonal metal, by Damiano and Herman (1959). The only apparent restriction on the packing is that the major axes of the plates must be parallel to the (0001) planes and the plates must pack themselves together in a regular array. Figure 13 also contains (D) a tracing of typical sub-plate packing from the 27.9 cm level of the ice sheet. Packing type B most closely describes the packing observed in the Point Barrow sea ice with the exception that the ends of the plates in the sea ice are more nearly rectangular in outline than hexagonal. Packing type C was occasionally observed over limited areas of a given thin section. Packing type A was never observed. There was no apparent systematic relation between the type of packing and the depth in the ice sheet.

ACKNOWLEDGEMENTS

The authors would like to thank Dr. A. Assur, Chief, Applied Research Branch, CRREL, for his interest and technical advice during the field

study and for critically reading the final manuscript. Mr. S. Nathenson kindly extended the use of the cold room facilities at the Arctic Research Laboratory, Point Barrow, Alaska.

References

ANDERSON, D. L. (1960), The physical constants of sea ice. *Research*, **13,** 310–318.

——— (1961), Growth rate of sea ice. *Jour. Glac.*, **3,** 1170–1172.

——— and W. F. WEEKS, (1958) A theoretical analysis of sea ice strength. *Trans. Am. Geophys. Union*, **39,** 632–640.

ASSUR, A. (1958) Composition of sea ice and its tensile strength: *Nat. Acad. Sci.-Nat. Res. Council Pub.* **598,** "Arctic Sea Ice," 106–138.

DAMIANO, V. AND M. HERMAN (1959) Cellular substructure in Zn crystals grown from the melt. *Trans. Met. Soc. AIME*, **215,** 136–138.

ELBAUM, C. (1959), Substructures in crystals grown from the melt. *Prog. Metal Physics*, **8,** 203–253.

FRANK, F. C. (1956), The origin of dislocations in crystals grown from the melt. IUTAM Colloq. (Madrid), *Deformation and Flow of Solids*, Springer-Verlag, Berlin, 73–78.

HALLETT, J. (1960), Crystal growth and the formation of spikes in the surface of supercooled water. *Jour. Glac.*, **3,** 698–702.

HILLIG, W. B. (1958), The kinetics of freezing of ice in the direction perpendicular to the basal plane. In *Growth and Perfection of Crystals*, John Wiley & Sons, New York, 350–359.

LEBEDEV, V. V. (1938), Rost l'da v arkticheskikh rehakh i moriakh v zavisimosti ot otritsatel'nykh temperatur vozdukha (Growth of ice in Arctic rivers and seas in relation to negative air temperatures). *Problemy Arkitiki*, **5–6,** 9–25.

MEHL, R. F. AND W. C. HAGEL (1956), The austenite: pearlite reaction. *Prog. Metal Physics*, **6,** 74–134.

SCHWARZACHER, W. (1959), Pack-ice studies in the Arctic Ocean. *Jour. Geophys. Res.*, **64,** 2357–2367.

TEGHTSOONIAN, E. AND B. CHALMERS (1951), The macromosaic structure of tin single crystals. *Canad. Jour. Physics*, **29,** 370–381.

WALTON, D. AND B. CHALMERS (1959), The origin of the preferred orientation in the columnar zone of ingots. *Trans. Met. Soc. AIME*, **215,** 447–457.

WEEKS, W. F. (1962), The structure of sea and salt ice. *USA CRREL Research* Report (in prep.)

——— AND O. S. LEE (1958), Observations on the physical properties of sea ice at Hopedale, Labrador. *Arctic*, **11,** 135–155.

——— AND A. ASSUR (1962), Structural control of the vertical variation of the strength of sea and salt ice. *Proc. Endicott Conf. Eng. Glaciology*, W. D. Kingery, editor (in press).

Manuscript received, January 18, 1962.